

TURBINE DYNAMIC BEHAVIOUR AND EXPECTED FATIGUE RELIABILITY

Martin GAGNON*

Institut de recherche d'Hydro-Québec (IREQ), Canada

Denis THIBAUT

Institut de recherche d'Hydro-Québec (IREQ), Canada

ABSTRACT

There is a close link between the dynamic behaviour a turbine runner blade and its expected reliability. The stresses sustained by the structure during steady state operation and transient conditions dictate both the expected fatigue reliability and the rate at which it decreases. Using the data from the measurement campaign conducted by Hydro-Québec, we observe that two distinct types of dynamic behavior and that each type of dynamic behaviour can generate three possible reliability scenarios. In general, we should expect different combination of dynamic behaviour and reliability scenario for different location on the runner blade given that each location has a different level of inspection, response spectrum or set of materials properties. Using these distinctions in terms of dynamic behavior and reliability, our goal is to help maximize the life expectancy of turbine runner while minimizing the risk to both the operator and manufacturer. This paper will present an overview of our methodology, results and recommendation regarding fatigue reliability assessment of turbine runner.

KEYWORDS

Reliability, Dynamic behaviour, High Cycle Fatigue (HCF), Hydroelectric turbine, Response spectra

1. INTRODUCTION

The expected fatigue reliability of runner blades in hydroelectric turbines is highly sensitive to its dynamic behaviour during steady state operation and transient conditions. We have observed that no turbine runner has exactly the same dynamic behaviour. Nonetheless, current measured data show that some distinct types of behaviour can be observed. These types of behaviour dictate the response spectrum which in turn is used as an input to obtain the expected reliability and sensitivity to material properties [1]. Because we need a simplified representation of the reality which is a trade-off between model complexity and sufficient detailed result [2], our objective is to show that the previously defined LCF/HCF response spectrum model [3] might be too simple for fatigue reliability assessment. Distinction between types of behaviour must be made in order to issue relevant recommendation to maximize life expectancy and reliability.

* *Corresponding author:* Institut de recherche d'Hydro-Québec (IREQ), 1800 Boulevard Lionel Boulet, Varennes, Québec, J3X 1S1, Canada, phone: +1 450 962 8359, email: gagnon.martin@ireq.ca

First, we need to define failure. For hydroelectric turbine runner blades, we defined failure as the onset of High Cycle Fatigue (HCF). In this case the onset of HCF is the contribution to crack propagation of small amplitude stress cycles which are different from the high amplitude cycles irrespective of their frequency as defined by Nicholas, 2006 [4]. The high amplitude cycles are thus considered the low cycle fatigue (LCF) component of the response spectra. This means that every steady operating condition should have a dynamic range below the HCF onset threshold at any given time [3]. Such definition has far reaching implications regarding the influence of turbine dynamic behaviour on fatigue reliability. A good knowledge of these implications should help both operator and manufacturer optimize their practice regarding the equipment reliability.

The paper is structured as follows. First, the typical HCF/LCF response spectra and the reliability model are presented. Next, we propose different types of dynamic behaviour based on the observed data from in situ measurements followed by a discussion on the expected fatigue reliability. Finally, specific guidelines and recommendations are suggested.

2. TURBINE RUNNER FATIGUE RELIABILITY

In previous work [3, 5, 6], we defined that, at any given point in time, the criteria for hydroelectric turbine runner fatigue reliability was that every allowed steady state operation should have a response spectrum below the HCF onset threshold. This means that, as the defect grows, the stress cycles range should stay below the limit formed by the Kitagawa diagram. The fatigue reliability limit state is illustrated in Fig. 1a. The simplest spectrum considered is composed of at least a high amplitude LCF component which contributes to crack propagation and some HCF components which should not contribute to propagation as shown in Fig. 1b. Notice the arrow in Fig. 1a which represents the movement toward the limit state of the joint distribution formed by the HCF stress range $\Delta\sigma$ and defect size a as the LCF component contributes to the crack propagation. This growth is a function of the number of LCF cycles happening with time.

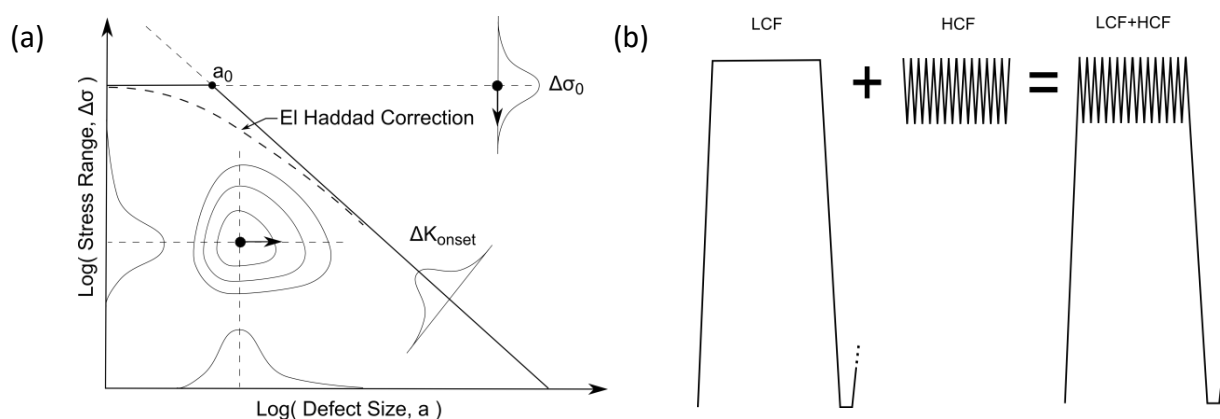


Fig. 1 (a) Fatigue reliability limit state; (b) Structure response spectrum.

The Kitagawa diagram [7] combines two limits ($\Delta\sigma_0$ and ΔK_{onset}) that are joined together using the El Haddad correction [8]. The limit state is expressed as follows:

$$g(a, \Delta\sigma) = \Delta\sigma - \frac{\Delta K_{onset}}{\sqrt{\pi(a+a_0)} Y(a+a_0)} \quad (1)$$

$$a_0 = \frac{1}{\pi} \left(\frac{\Delta K_{onset}}{\Delta\sigma_0 Y(a_0)} \right)^2 \quad (2)$$

Often, ΔK_{th} is used in place of ΔK_{onset} because it is easier to measure hence more readily available. For the following discussion, we will only use ΔK_{th} . From Eq. 1, we obtain the probability of failure P_f by solving the following:

$$P_f = \int_{g(x) \leq 0} f_X(x) dx \quad (3)$$

in which, x is an n -dimensional vector of random variables with a joint density function $f_X(x)$. This value can easily be approximated using First Order Reliability Methods (FORM) as describe in [3]. The results can either be expressed in terms of the reliability index β , probability of failure P_f or runner reliability R as follows:

$$P_f = \Phi(-\beta) \quad (4)$$

$$R = (1 - P_f)^n \quad (5)$$

where n is the number of blades of the runner and $\Phi(\cdot)$ is the standard normal cumulative distribution function. Notice that from this definition HCF will occur when the largest defect in a given volume propagates due to the largest stress cycle of a given return period. Hence, the uncertainty around the defect size and stress range should be modelled using an extreme value distribution. In our case, we have chosen to use the Gumbel distribution for simplicity purpose. Furthermore, unless mentioned otherwise the parameters in Table 1 are used to illustrate the limit state in this paper. Those parameters represent the limit below which we believe we are completely safe and above which we are certain that the onset of HCF has occurred in CA6NM stainless steel [6].

Parameters	Uncertainty interval	Units
ΔK_{th}	[2.0, 4.0]	MPa·m ^{1/2}
$\Delta \sigma_0$	[55, 550]	MPa

Tab. 1. Limit state parameters uncertainty interval

3. DYNAMIC BEHAVIOUR TYPE 1

Dynamic behaviour type 1, while similar to the response spectrum presented in Fig. 1b, includes the transient due to the startup, shutdown and major load changes. This type of behaviour was first presented in [5] and is shown in Fig. 2. Such behaviour is suitable for a wide range of runner ranging from Francis to propeller type. Notice that the transients' amplitudes can be optimized and are not fixed [9]. The characteristics needed to generate a suitable simplified response spectrum are the following:

- The maximum stress range of the startup transient.
- The maximum stress range of the shutdown transient.
- The frequency of startup/shutdown.
- The maximum stress ranges generated by each major load change.
- The frequency of each major load change.
- The maximum stress range of the critical steady state regime.

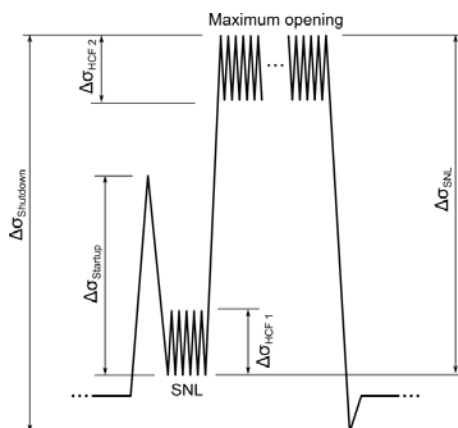


Fig. 2. Type 1 simplified response spectrum.

Two distinct possibilities can be observed. We can either observe $\Delta\sigma_{HCF1} \leq \Delta\sigma_{HCF2}$ or $\Delta\sigma_{HCF1} > \Delta\sigma_{HCF2}$. These two possibilities generate 3 different cases in term of reliability:

- Case 1: $\Delta\sigma_{HCF1} \leq \Delta\sigma_{HCF2}$
- Case 2: $\Delta\sigma_{HCF1} > \Delta\sigma_{HCF2}$ and both stress ranges within the allowed limits
- Case 3: $\Delta\sigma_{HCF1} > \Delta\sigma_{HCF2}$ and $\Delta\sigma_{HCF1}$ outside the allowed limit

Fig. 3 shows two examples of measured data which belong to type 1 case 1 response. In case 1 since $\Delta\sigma_{HCF2}$ will always be the first stress range to reach the threshold defined by our limit state. Hence, we can neglect $\Delta\sigma_{HCF1}$ which simplify the reliability analysis as shown in Fig. 4.

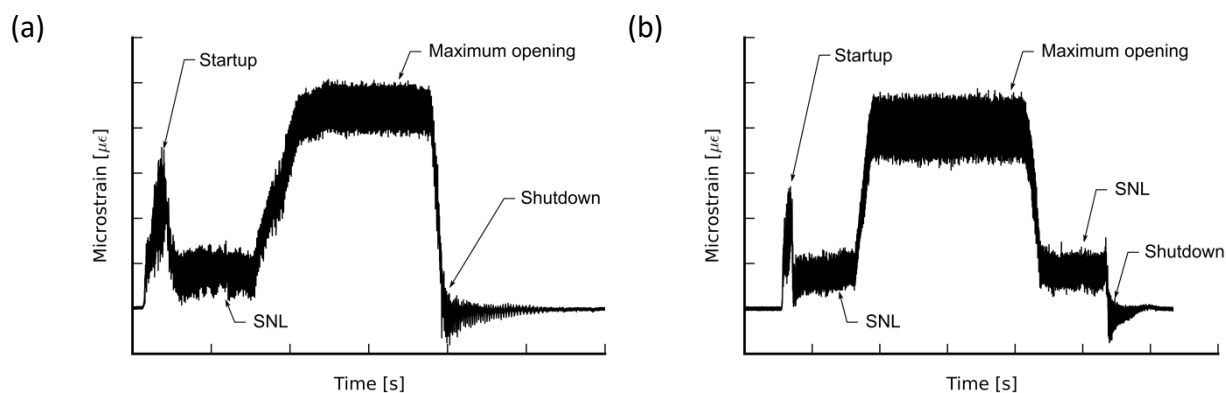


Fig. 3 Two measured examples of type 1 case 1 response.

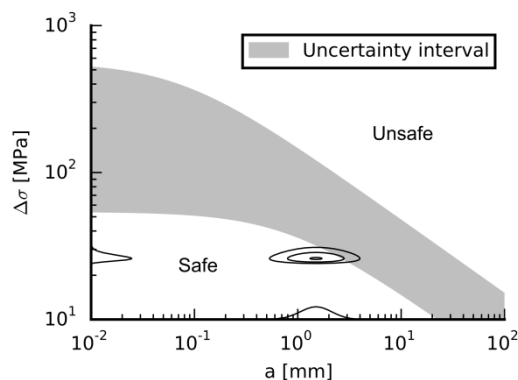


Fig. 4 Example of type case 1 reliability problem.

However this is not always true as shown in Fig. 5. Sometime, we cannot neglect $\Delta\sigma_{HCF1}$. In such situation, we are either in case 2 or case 3 as shown in Fig. 6. In case 2, when $\Delta\sigma_{HCF1}$ reach the limit state, rather than failure we move to case 3 where we need to account for the number of $\Delta\sigma_{HCF1}$ cycles N_{HCF1} contributing to crack propagation within every start to stop cycle.

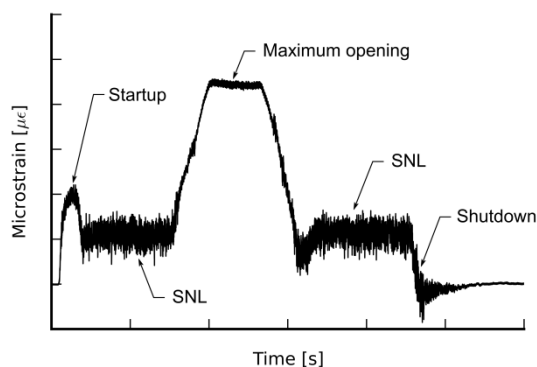


Fig. 5 A measured example of type 1 case 2 response.

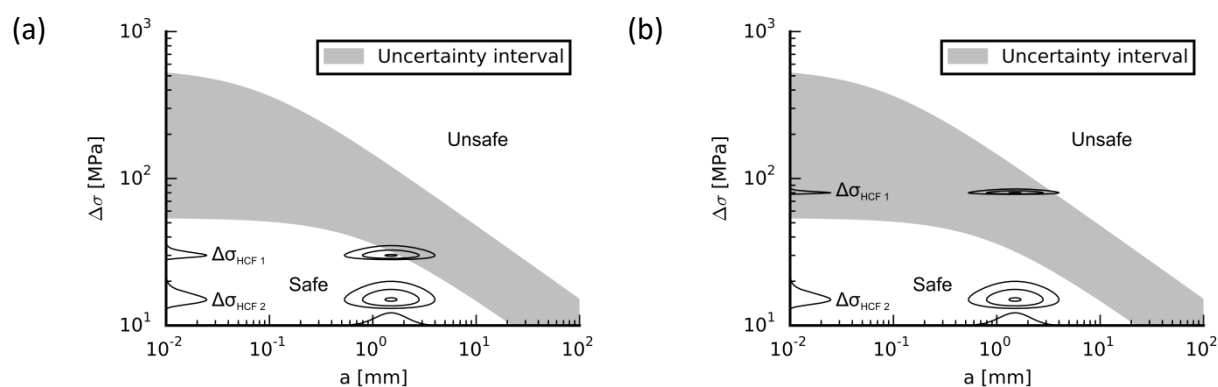


Fig. 6 (a) Case 2 with all operating condition safe; (b) Case 3 with some operating condition unsafe.

4. DYNAMIC BEHAVIOUR TYPE 2

Type 1 is not the only behaviour observed; at the critical location on some turbine runners, the behaviour presented in Fig. 7 is observed. Such behaviour is characterized by maximum stress at the SNL condition rather than maximum opening. The consequence is more LCF cycles because we need to go twice thru the SNL condition: once during the startup and once during the shutdown of the unit. Hence with the type 2 response spectrum even if we can neglect the startup and shutdown transients, we still have twice the amount of LCF cycles. This means less time in the safe region for any of the 3 cases presented.

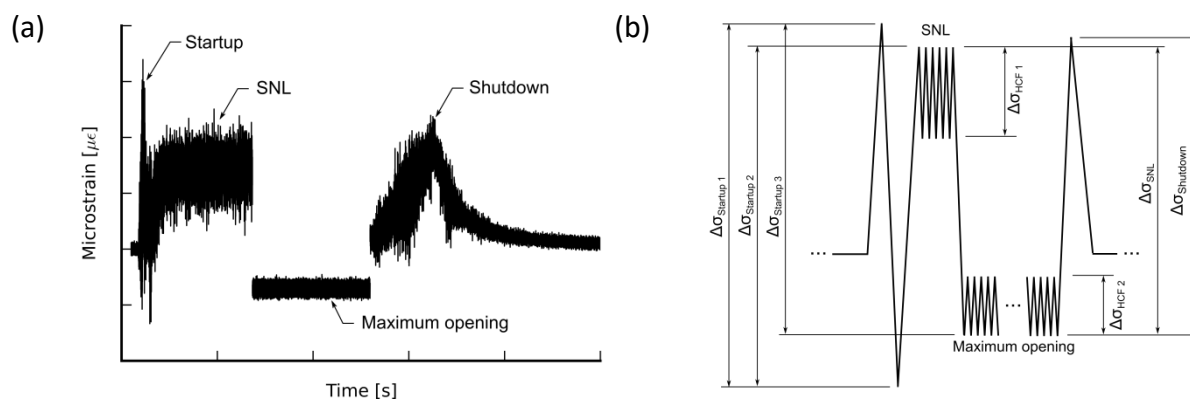


Fig. 7 (a) Measured example of Type 2 response; (b) Type 2 simplified response spectrum.

5. DISCUSSION

The main difficulty is that we cannot limit our analysis of reliability to only one location. In general, we should expect that not all locations have the same level of inspection, response spectrum or materials properties. Furthermore, when we have a combination of parameters that generate case 3, the reliability will not only be sensitive to the number of start-stop cycles and stress amplitudes but also become highly sensitive to the time of operation in a given operating condition. To illustrate this difficulty, we used the parameters in Tab. 2 to generate three results presented in Fig. 8a. Here, the rate at which reliability decreases is highly sensitive to the number of HCF cycles N_{HCF1} which is a function of the time of operation in this operating condition. This sensitivity is only one aspect, notice that as more and more stress cycles of lower amplitude from this operating condition reach the limit state, we might need at some point to account for the complete dynamic content rather than only its extreme values. The use of a complete stochastic simulation for the desired length of time would provide more accurate results but increases significantly the model complexity [10].

Parameters	Location	Scale	Distribution type	Units
a	1.5	0.5	Gumbel	mm
$\Delta\sigma_{HCF1}$	80.0	1.0	Gumbel	MPa
$\Delta\sigma_{HCF2}$	15.0	[0.5, 1.0*, 2.0]	Gumbel	MPa
$\Delta\sigma_{SNL}$	200.0	-	-	MPa
$N_{Startup}$	1	-	-	Day ⁻¹
N_{HCF1}	[0, 10*, 100]	-	-	Startup ⁻¹

* value used unless specified otherwise

Tab. 2 Parameter values for case 3 sensitivity analysis.

Another aspect often overlooked is the uncertainty around the stress range for steady state operation. In Fig.8b, we varied the uncertainty around the value of $\Delta\sigma_{HCF2}$ for $N_{HCF1} = 10$. Here, the scale of the distribution is the parameter related to the dispersion or uncertainty. We observe that if we lower the uncertainty below a certain level, the initial reliability will increase but given the decreasing rate for $N_{HCF1} = 10$ it will have a limited impact as time goes by. On the other hand, if the uncertainty is large, the impact will be significant across the whole range of values. This shows that a reduction of stress level uncertainty can have as much influence in terms of reliability as reducing the expected value itself. However, below a

certain level a reduction of uncertainty provides limited gains. This is one of the main justifications behind in situ measurement campaign on runner prototype.

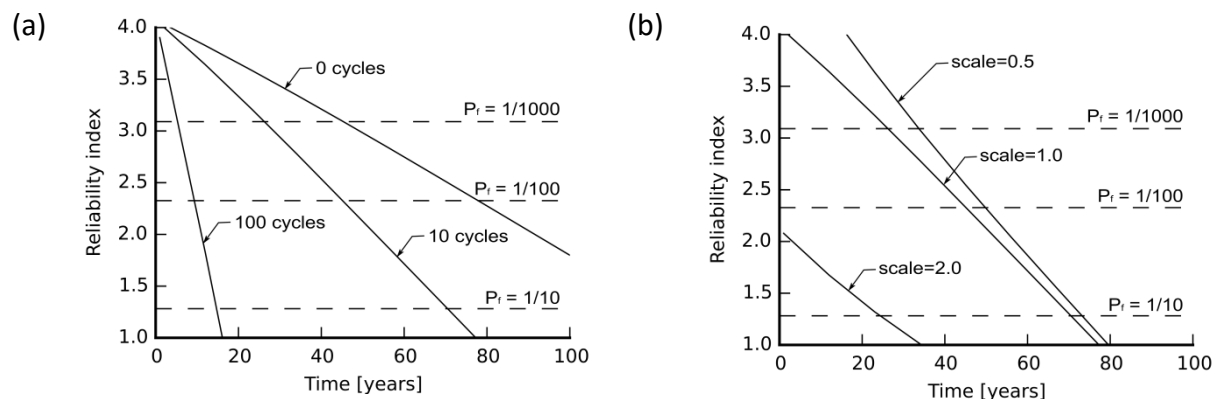


Fig. 8 Case 3 sensitivity analysis; (a) Number of cycle N_{HCF1} ; (b) $\Delta\sigma_{HCF2}$ uncertainty (i.e.: scale).

6. CONCLUSION

In this paper, we have identified 2 types of response spectrum to represent the dynamic behaviour observed in hydroelectric turbine runners from our measurement campaigns. The first type of response spectrum tends to warrant higher reliability since the second type of dynamic behaviour generates more LCF cycles. Compared to the first type of behaviour, the second type would have a higher expected reliability decreasing rate for similar parameter values. For each of these response spectrums, 3 scenarios have been identified:

- Case 1: $\Delta\sigma_{HCF1} \leq \Delta\sigma_{HCF2}$
- Case 2: $\Delta\sigma_{HCF1} > \Delta\sigma_{HCF2}$ and both stress range in the safe region
- Case 3: $\Delta\sigma_{HCF1} > \Delta\sigma_{HCF2}$ and $\Delta\sigma_{HCF1}$ not in the safe region

Our recommendation are that regardless of the type of spectrum if the decreasing rate is low and high reliability can be expected, one should still do periodic visual inspection to ensure that no error or unexpected events occurred. The reliability decreasing rate is controlled by the LCF cycles and number of start to stop cycles. When it becomes significant, we will reach a point where the inspection is the only way to ensure that there is no cracking. For such runner, rigorous inspection schedule should be respected to maintain a given reliability level. However, one should remember that the inspection of the runner is not the only way to improve reliability. A better knowledge of material properties or stress level could achieve the same goal. Hence, stress measurements campaigns and a better knowledge of the specific material properties of a given runner are tools we can use to minimize the risk of runner blade cracking.

7. REFERENCES

- [1] Thibault, D., Gagnon, M. & Godin, S.: Bridging the gap between metallurgy and fatigue reliability of hydraulic turbine runners. *IAHR 27th Symposium on Hydraulic Machinery and Systems*. Montreal. 2014.
- [2] Aven, T.: *Foundations of Risk Analysis*, 2nd Edition. John Wiley & Sons. 2012.
- [3] Gagnon, M., Tahan, A., Bocher, P. & Thibault, D.: A probabilistic model for the onset of High Cycle Fatigue (HCF) crack propagation: Application to hydroelectric turbine runner. *Int. J. Fatigue*. 47 (2013) 300-7.

- [4] Nicholas, T.: *High Cycle Fatigue: A Mechanics of Materials Perspective*. Elsevier. 2006.
- [5] Gagnon, Tahan, M. A., Bocher, P. & Thibault, D.: Influence of load spectrum assumptions on the expected reliability of hydroelectric turbines: A case study. *Structural Safety*. 50 (2014) 1-8.
- [6] Gagnon, M., Tahan, A., Bocher, P. & Thibault, D.: On the Fatigue Reliability of Hydroelectric Francis Runners. *Procedia Engineering*. 66 (2013) 565-574.
- [7] Kitagawa, H. & Takahashi, S.: Applicability of fracture mechanics to very small cracks or the cracks in the early stage. *Second International Conference on Mechanical Behavior of Materials*. ASM. Metals Park. Ohio. 1976. 627-31.
- [8] El Haddad, M.H., Topper, T. & Smith, K.: Prediction of non propagating cracks. *Eng. Fract. Mech.* 11 (1979) 573–84.
- [9] Gagnon, M., Jobidon, N., Lawrence M. & Larouche, D.: Optimization of turbine startup: Some experimental results from a propeller runner. *IAHR 27th Symposium on Hydraulic Machinery and Systems*. Montreal. 2014.
- [10] Poirier, M.: *Modélisation et simulation du comportement dynamique des aubes de turbines hydroélectriques*, École de technologie supérieure, Université du Québec, Master's thesis, 2013.

8. NOMENCLATURE

a	defect size	ΔK_{th}	stress intensity factor of the LEFM threshold
a_0	defect size at which the fatigue limit and the LEFM threshold cross	ΔK_{onset}	stress intensity factor of the HCF onset
$f_x(x)$	joint density function	$\Delta\sigma$	stress cycle range
$g(x)$	limit state	$\Delta\sigma_0$	fatigue limit
n	number of blades	$\Delta\sigma_{LCF}$	stress cycle range of the LCF loading component
t	time	$\Delta\sigma_{HCF}$	stress cycle range of the HCF loading component
x	an n-dimensional vector of random variables	$\Delta\sigma_{Shutdown}$	stress cycle range of the shutdown transient
$Y(a)$	stress intensity correction factor for a given geometry	$\Delta\sigma_{SNL}$	stress cycle range of the regime change from maximum opening to SNL
ΔK	stress intensity factor	$\Delta\sigma_{Startup}$	stress cycle range of the startup transient